Karol NAJDEK[1], Radosław NALEPA[1], Marcin ZYGMANOWSKI[2]

Wroclaw University of Scientist and Technology (1), Silesian University of Technology (2)

Identification of Dual-Active-Bridge converter transfer function

Abstract. Frequency-domain identification method of the Dual-Active-Bridge converter control-to-output and closed loop control transmittances by means of the Matlab (tfest function) is presented in this paper. The phase shift modulation is used as the converter control scheme. The closed loop control was designed basing exclusively on the estimated control-to-output (the control object) transfer function. Presented experimental and computer simulation results are in form of the Bode plots and the output voltage step responses.

*Streszczenie. W artykule zaprezentowano metodę częstotliwościową do identyfikacji transmitancji podwójnego mostka H z wykorzystaniem pakietu Matlab (tfest funkcja) - zarówno samego członu energoelektronicznego, jako obiektu regulacji przy zmianie kąta przesunięcia pomiędzy stroną pierwotną i wtórną, jak i kompletnego zamkniętego układu regulacji napięcia wyjściowego. Zamknięty układ regulacji zaprojektowano wyłącznie na podstawie estymowanej transmitancji obiektu. W artkule zaprezentowano wyniki eksperymentalne wraz z wynikami z modelu symulacyjnego, w formie charakterystyk amplitudowo-fazowych oraz odpowiedzi na skok jednostkowy.(**Identyfikacja transmitancji konwertera z podwójnym mostkiem aktywnym**)*

Keywords: dual active bridge, object identification, frequency-domain identification
Słowa kluczowe: podwójny mostek H, identyfikacja obiektu, identyfikacja częstotliwościowa

Introduction

Nowadays electric power conversion circuits are basing on power electronics, measurements and control solutions. All that combined together with widely available data exchange means creates foundation for advanced electric power conversion systems [1]. Such systems are complex and exposed to changing operating conditions. In addition they are quite often safety related.

In such case there is a real need for trustworthy solutions for fast and relatively easy transfer function identification of selected power system components (circuits). Knowledge of the transfer function helps to develop tailored control solutions dedicated to the real world circuits [2]. In such case selection of the control mechanism relies on sufficient set of information in given range of the dynamics, without compromise on relevant gains and time constants which may have direct impact on dynamic performance and stability.

There is a number of identification methods reported in literature [3], which could be used to identify miscellaneous systems. In this paper we concentrate on one of the fundamental methods basing on analysis in frequency domain [4]. The method is called Frequency Response Analysis, FRA, [3]. The sampled signal analyses are conducted with use of Matlab&Simulink environment.

As the identification object the Dual Active Bridge DC/DC converter, DAB, is used [5]. The circuit, see Fig.1, is considered as a promising power electronics building block solution for the solid state transformers, SST, [6, 7]. The SST is one of the key components of the future smart grids. Despite of relatively long circuit existence, since 80'ties, it is still considered as significant challenge in terms of design, mathematical modelling and digital control [6, 8].

In order to simplify the control design of such a circuit the frequency domain transfer function identification method is used to estimate control-to-output transfer function. Basing on the function, the controller type is selected - PI in this case. As next, the PI gains are selected and verified with an experimental setup. The circuit measurements are compared to developed simulation model results.

In this paper, as first the considered DAB circuit is presented. As next, the control-to-output transfer function is estimated basing on measurement points. This is followed by closed loop regulator selection and tune accompanied by a simulation model. In the end conclusions are given.

The Dual Active Bridge converter as the identification object

General block diagram of considered DAB converter can be seen in Fig.1. Its parameters can be seen in Table 1. The primary design objective was to create an experimental setup meant to be used for testing of chosen transfer function identification method.

The rated DC output voltage, $V_{DAB,out}^{rtd}$, was chosen to be equal to 30 V, and this with input rated voltage, $V_{DAB,in}^{rtd}$, set to 60 V. Maximum output power, $P_{DAB,out}^{max}$, was assumed as 80 W. The converter efficiency was not optimized during the design phase but aimed at near to 80%. The F450R12KS4 IGBT modules were used as the switching devices. As the signal processing and control platform the STM32F4-Discovery board with a 12 bit A/D converter was used. The switching frequency was set to constant value of 16 kHz.
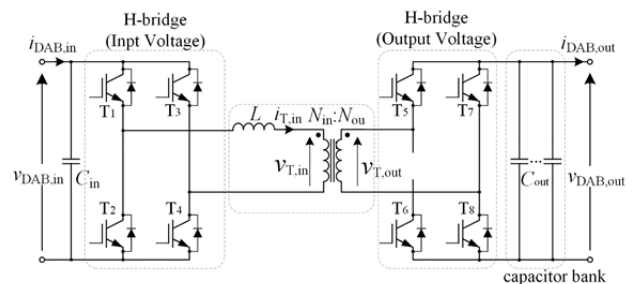

Fig.1. Dual Active Bridge, DAB, general circuit diagram

As the DAB power transfer control method the Single Phase Shift modulation, SPS, was used [7, 8]. The method is basing on variation of the phase shift, φ_{out}, between the input voltage side, $v_{DAB,in}$, and the output voltage side, $v_{DAB,out}$, gate drive signals. The duty cycle of all the gate drive signals, D_{in} and D_{out}, is set to 50 %. The dead time , T_{dt}, of 1 μs is applied between the upper and the lower signals in order to avoid the short circuits in between switching. By changing the phase shift, the power transfer is controlled basing on variation of the L inductance current, i_L, which is the same as the input transformer current $i_{T,in}$, see drawing in Fig.2. Apart from the control method used, there are also different control methods. They rely on duty cycles variations of the input and output side transistors [7]. It is in addition to the φ_{out} variation. Most recently there are also further extensions of the control methods aiming at

reduction of the DC-bias transformer current [9, 10] and the converter efficiency increase at low load [11].
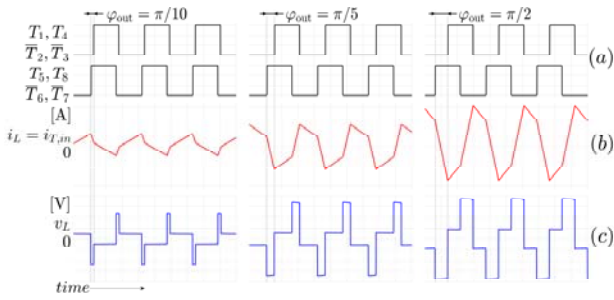

Fig.2. Phase Shift Modulation, PSM, control principle visualization at three different phase shifts, $\varphi_{\text{out}} \in \left\{ \frac{\pi}{10}, \frac{\pi}{5}, \frac{\pi}{2} \right\}$ accordingly: a) gate drive signals of IGBT transistors as per Fig.1, b) L inductance current, c) voltage across the L inductance

Developed test circuit was verified through measurement of its output power within assumed output voltage, $v_{DAB,out}$, tolerance (±10 %) in function of the φ_{out}. The results can be seen in Fig.3. They are combined with theoretical curves calculated according to the following equation (1):

$$(1) \qquad P_{\text{DAB}} = \frac{V_{\text{DAB,in}} V_{\text{DAB,out}} n \varphi_{\text{out}} \left(\pi - |\varphi_{\text{out}}| \right)}{2\pi^2 f_s L}$$

where: P_{DAB} – DAB power transfer [W] assuming lossless conversion; $V_{\text{DAB,in}}$, $V_{\text{DAB,out}}$ – input and output voltages respectively [V]; n – the transformer turns ratio; φ_{out} – output voltage side phase shift angle [rad]; L – total DAB inductance; f_s = 16 kHz is the switching frequency [Hz].
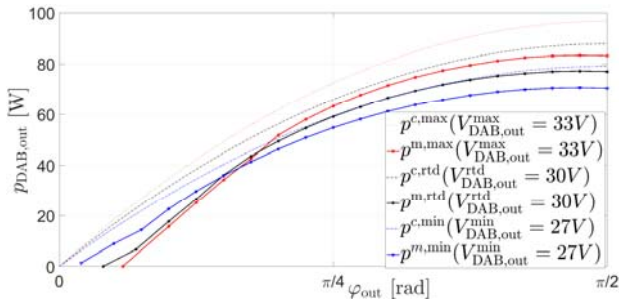

Fig.3. The DAB converter power transfer characteristics measured in laboratory, p^{m}, and calculated according to equation (1), p^{c}, as functions of the φ_{out}. Plots are drawn for L = 320 μH and $V_{\text{DAB,in}}$ = 60 V, the $V_{\text{DAB,out}}$ are given in the plot legend

The theoretical characteristics from Fig.3 are above the measured ones because the equation (1) does not take into account the real converter efficiency. In addition, one should notice that the measured characteristics do not start from zero power at $\varphi_{\text{out}} = 0$ rad. The main contributor to that is the dead time T_{dt} analyzed in details in [7, 12]. The maximum measured output power at $V_{\text{DAB,out}}^{\text{rtd}}$ = 30 V is $p^{\text{m,rtd}}$= 77 W which is near enough to the assumed 80 W.

Measured efficiency of the tested circuit can be seen in Fig.4. It exceeds 80 % in the output power range of 9 W to 63 W. Nowadays it is not a satisfactory result for commercial products. Nevertheless such optimization was not assumed as task for this research and is not a subject to this paper. One should only notice that the DAB converter efficiency optimization is a complex multivariable optimization effort. Up to date research results report about 95 % as the high end [12, 13].
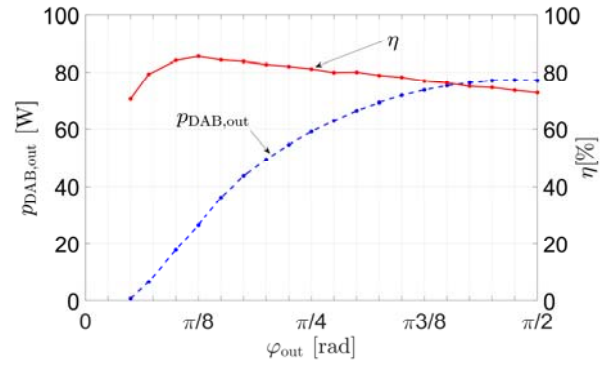

Fig.4. Laboratory measured investigated DAB converter efficiency shown together with the output power at $V_{\text{DAB,out}}$ = 30 V. Measurements conducted at $V_{\text{DAB,in}}$ = 60 V

Identification of the control-to-output transfer function

The experimental circuit control-to-output transfer function, $TF_{\text{DAB}}^{\text{exp,c2o}}$, was identified basing on measurements conducted according to general block diagram shown in Fig.5, configuration No. I. The measurements were done for selected steady state phase shift reference point, $\varphi_{\text{out}}^{\text{ref}}$ = $\pi/4$, summed with changed frequency sinusoidal disturbance $\tilde{\varphi}_{\text{out}}^{\text{ref}}$ causing ± 1 V$^{\text{pk}}$ variation of the v_{out} at the initially low frequency. The $\tilde{\varphi}_{\text{out}}^{\text{ref}}$ frequency was in range of 0.1 Hz to 2 kHz and changed in steps as shown in Fig. 6 for measured magnitude and phase, $TF_{\text{DAB}}^{\text{exp,m,c2o}}$.
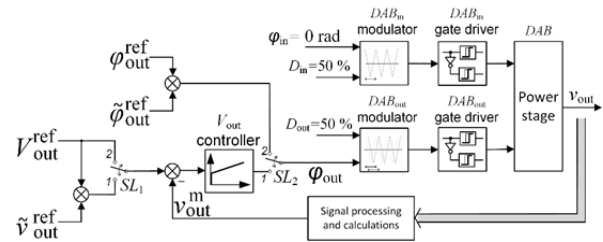

Fig.5. General overview of: No. I - the control-to-output transfer function, $TF_{\text{DAB}}^{\text{exp,c2o}}$, identification with selector SL_2 in position 2; No. II - the closed loop reference-to-output transfer function, $TF_{\text{DAB}}^{\text{exp,r2o}}$, identification with SL_1 and SL_2 in position 1; No. III - the closed loop control tests with SL_1 in position 2 and SL_2 in position 1

The measured points marked in Fig. 6, were used in Matlab (*tfest* function) to estimate following control-to-output transfer function equation:

$$(2) \qquad TF_{\text{DAB}}^{\text{exp,est,c2o}}(s) = \frac{19.088}{0.039s + 1}$$

The equation (2) was estimated with fit to the estimation data equal to 96.3 % and its Bode plot together with the measured data points can be seen in Fig. 6. The magnitude decrease by 3 dB point is located at frequency of 4 Hz. The estimated transfer function was also verified through comparison of the calculated/simulated and the experimentally measured step response of the output voltage to the phase shift command at time of 0.1 s, see Fig. 7. Obtained results indicate sufficient accuracy of the equation (2) and therefore it was used as the object transfer function during the output voltage closed loop control design.
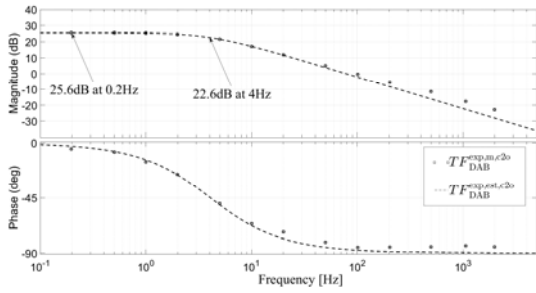
Fig. 6. The Bode plot of control-to-output transfer function experimentally measured points, $TF_{DAB}^{exp,m,c2o}$, and estimated equation (2), $TF_{DAB}^{exp,est,c2o}$
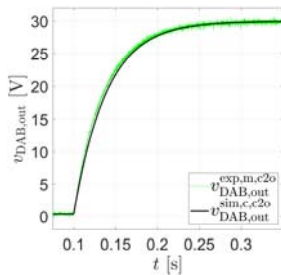

Fig. 7. Step response of (control-to-output) experimentally measured, $v_{DAB,out}^{exp,m,c2o}$, and simulated, $v_{DAB,out}^{sim,m,c2o}$, converter output voltage, at phase shift reference step command $\varphi_{out}^{ref} = \pi/4$, at time of 0.1 s, with sampling time of 31.25μs and 16 kHz switching frequency

Closed loop control of the DAB converter output voltage

Basing on the estimated continuous time object transfer function (2), $TF_{DAB}^{exp,est,c20}$, a basic discrete time PI regulator was selected to control the DAB converter output voltage. The proportional, K_P, and integral, K_I, gains values, see Table 2, were selected experimentally basing on few simulation model runs. For purpose of the simulations the $TF_{DAB}^{exp,est,c20}$ was converted to the discrete time domain with sampling time of 31.25 μs (twice the PWM frequency, f_s). The selected gains were verified with the experimental setup according to Fig.5, configuration No. III.

Basing on measured data points, following estimated closed loop reference-to-output transfer function was obtained:

$$(3) \qquad TF_{DAB}^{exp,est,r2o}(s) = \frac{181.6s - 2283}{s^2 + 158.8s - 2330}$$

The equation (3) assures fit to the estimation data equal to 92.4 %. In addition to this transfer function, another estimate was conducted with the discrete time simulation model – just as verification of the estimation mechanism used. Basing on data points obtained from the simulation, following transfer function was found with fit to the estimation data equal to 99.88 %

$$(4) \qquad TF_{DAB}^{sim,est,r2o}(s) = \frac{168.5s + 9086}{s^2 + 194.4s + 9085}$$

Such high estimation fit is due to the clearly defined identification object and lack of the measurement noise present in the real circuit.

Obtained by measurements and simulation data points together with the estimated closed loop transfer functions'

Bode plots can be seen in Fig. 8. The results are sufficiently convergent. Small discrepancy in phases is caused by lack of delays associated with the real time computing and lack of measurement noise in deliberately simplified simulation model. The -3dB point in Fig. 8 is at 30 Hz instead of the 4 Hz indicated in Fig. 6.
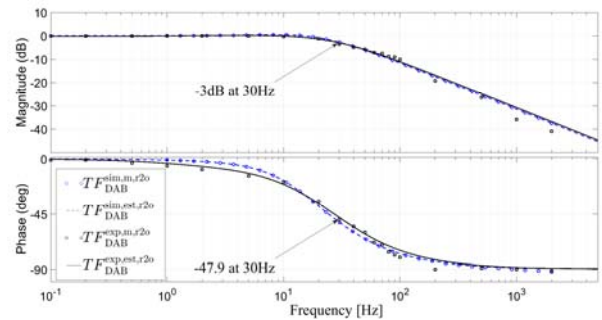

Fig. 8. The Bode plots of closed loop reference-to-output transfer functions experimentally measured data points, $TF_{DAB}^{exp,m,r2o}$, and simulated data points, $TF_{DAB}^{sim,m,r2o}$, together with results from the estimated equations (3), $TF_{DAB}^{exp,est,r2o}$, and (4), $TF_{DAB}^{sim,est,r2o}$, with K_P = 0.314 rad/V and K_I = 8.376 rad/V*s

Similarly like for the control-to-output case, the estimated reference-to-output transfer function was verified by comparison of the output voltage step responses to the reference command at time of 0.1 s, see Fig. 9. Results shown in Fig. 9 a) are with the PI regulator gains set to avoid the output voltage overshoot and they are corresponding to the Bode plots shown in Fig. 8. Results with more aggressive PI tuning can be seen in Fig. 9 b). There is slightly faster reference voltage reach on expense of about 15 % overshoot without loss of stability.
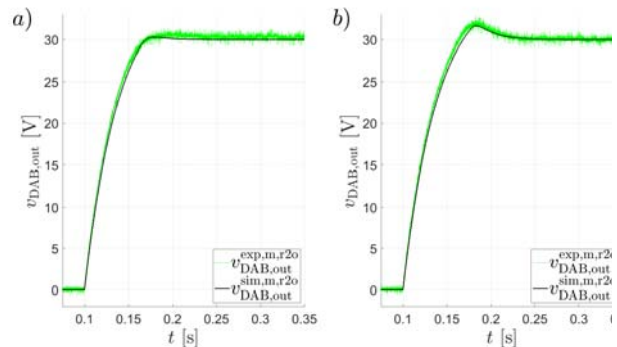

Fig. 9. Closed loop control step responses of (reference-to-output) experimentally measured, $v_{DAB,out}^{exp,m,r2o}$, and simulated, $v_{DAB,out}^{sim,m,r2o}$, converter output voltage, at the voltage reference step command V_{out}^{ref} = 30 V, at time of 0.1 s, with sampling time of 31.25μs and 16 kHz switching frequency, with the PI regulator gains: a) K_P = 0.314 rad/V, K_I = 8.376 rad/V*s; b) K_P = 0.262 rad/V, K_I = 16.755 rad/V*s

The closed loop regulator tuning in the presented case was conducted basing exclusively on an identified object transfer function, without any parametric modeling. Estimated transfer functions are sufficient for both to tune the regulator and to develop simplified mathematical/simulation models.

Conclusion/Summary

Identification method basing on the frequency-domain has been successfully applied to the Dual-Active-Bridge converter transfer function determination.

The identified transfer function has been used to design the output voltage closed loop control with a PI

compensator. The PI gains firstly have been selected through simulation in Matlab-Simulink environment and secondly verified with a prototype in laboratory.

Obtained experimental results confirm usefulness of the frequency response analysis (FRA) method to identify mathematical models of advanced power electronics converters such as DAB.

Further research will be carried on identification of the circuit in conjunction with the nearest surrounding system components including nonlinearities.

Table 1. Parameters of the DAB circuit

Parameter Name	Value
Input rated voltage, $V_{DAB,in}^{rtd}$	60 VDC
Output rated voltage, $V_{DAB,out}^{rtd}$	30 VDC
Output voltage tolerance, $V_{DAB,out}^{tol}$	± 10 %
Converter inductance, L	320 µH
Input capacitance, C_{in}	1.5 mF
Output capacitance, C_{out}	4 mF
Transformer turn ratio, n	2
Switching frequency, f_s	16 kHz
Assumed efficiency, η_{DAB}	80 %
Gate drive dead time, T_{dt}	1 µs

Table 2. The DAB output voltage regulator gains

Parameter Name	Value
Proportional gain – basic, K_P	0.314 rad/V
Integral gain - basic, K_I	8.376 rad/V*s
Proportional gain – overshoot, K_P	0.262 rad/V
Integral gain - overshoot, K_I	16.755 rad/V*s

Authors: *mgr inż. Karol Najdek, Politechnika Wrocławska, Wydział Elektryczny, Katedra Energoelektryki, Wybrzeże Wyspiańskiego 27, 50-370 Wrocław, E-mail: karol.najdek@pwr.edu.pl; dr inż. Radosław Nalepa, Politechnika Wrocławska, Wydział Elektryczny, Katedra Energoelektryki, Wybrzeże Wyspiańskiego 27, 50-370 Wrocław, E-mail: radoslaw.nalepa@pwr.edu.pl; dr inż. Marcin Zygmanowski, Politechnika Śląska, KENER, ul. B. Krzywoustego, 44-100, E-mail: marcin.zygmanowski@polsl.pl.*

REFERENCES

[1] Boroyevich D., Cvetkovic I., Burgos R., and Dong D., Intergrid: A Future Electronic Energy Network?, *IEEE Journal of Emerging and Selected Topics in Power Electronics*, 2013, vol. 1, no. 3, pp. 127-138.
[2] Franklin G. F. and Powell J. D., Digital control of dynamic systems, *Addison-Wesly Publishing Company,* 1980.
[3] Nelles O., Nonlinear System Identification, *Springer-Verlag Berlin Heidelberg,* 2001.
[4] Pintelon R., Guillaume P., Rolain Y., Schoukens J., and Hamme H. V., Parametric identification of transfer functions in the frequency domain-a survey, *IEEE Transactions on Automatic Control*, 1994, vol. 39, no. 11, pp. 2245-2260.
[5] Doncker R. W. A. A. D., Divan D. M., and Kheraluwala M. H., A three-phase soft-switched high-power-density DC/DC converter for high-power applications, *IEEE Transactions on Industry Applications*, 1991, vol. 27, no. 1, pp. 63-73.
[6] Huber J. E. and Kolar J. W., Analysis and design of fixed voltage transfer ratio DC/DC converter cells for phase-modular solid-state transformers, in *2015 IEEE Energy Conversion Congress and Exposition (ECCE)*, 2015, pp. 5021-5029.
[7] Zhao B., Song Q., Liu W., and Sun Y., Overview of Dual-Active-Bridge Isolated Bidirectional DC-DC Converter for High-Frequency-Link Power-Conversion System, *IEEE Transactions on Power Electronics*, 2014, vol. 29, no. 8, pp. 4091-4106.
[8] Ling S., Wanjun L., Jun H., Zhuoqiang L., Yao C., and Yue W., Full discrete-time modeling and stability analysis of the digital controlled dual active bridge converter, in *2016 IEEE 8th International Power Electronics and Motion Control Conference (IPEMC-ECCE Asia)*, 2016, pp. 3813-3817.
[9] Nalepa R., Zygmanowski M., and Michalik J., Dual-Active-Bridge converter inductance DC-bias current compensation under low and high load conditions, *Przegląd Elektrotechniczny*, 2018, no. 07, pp. 1-5.
[10] Zhao B., Song Q., Liu W., and Zhao Y., Transient DC Bias and Current Impact Effects of High-Frequency-Isolated Bidirectional DC-DC Converter in Practice, *IEEE Transactions on Power Electronics*, 2016, vol. 31, no. 4, pp. 3203-3216.
[11] Oggier G. G. and Ordonez M., High-Efficiency DAB Converter Using Switching Sequences and Burst Mode, *IEEE Transactions on Power Electronics*, 2016, vol. 31, no. 3, pp. 2069-2082.
[12] Barlik R., Nowak. M., Grzejszczak P., Power transfer analysis in a single phase dual active bridge, *Bulletin of Polish Academy of Science, Technical Sciences*, 2013, vol. 61, no. 4, p. 20.
[13] Krismer F. and Kolar J. W., Efficiency-Optimized High-Current Dual Active Bridge Converter for Automotive Applications, *IEEE Transactions on Industrial Electronics*, 2012, vol. 59, no. 7, pp. 2745-2760.